Supporting information

Observation of surface species in plasma-catalytic dry reforming of methane in a novel atmospheric pressure dielectric barrier discharge *in situ* IR cell

Joran VAN TURNHOUT[a,b] , Domenico ACETO[b,c], Arnaud TRAVERT[b], Philippe BAZIN[b], Frédéric Thibault-Starzyk[b], Annemie BOGAERTS[a] and Federico AZZOLINA-JURY[b,*]

a Research group PLASMANT, Department of Chemistry, University of Antwerp, Universiteitsplein 1, BE-2610 Wilrijk-Antwerp, Belgium

b Normandie Univ, ENSICAEN, UNICAEN, CNRS, Laboratoire Catalyse et Spectrochimie (LCS), 14000 Caen, France

c CQE-DEQ, Instituto Superior Técnico, Universidade de Lisboa, 1049-001 Lisboa, Portugal

* Corresponding author

S1. Experimental setup: additional figures

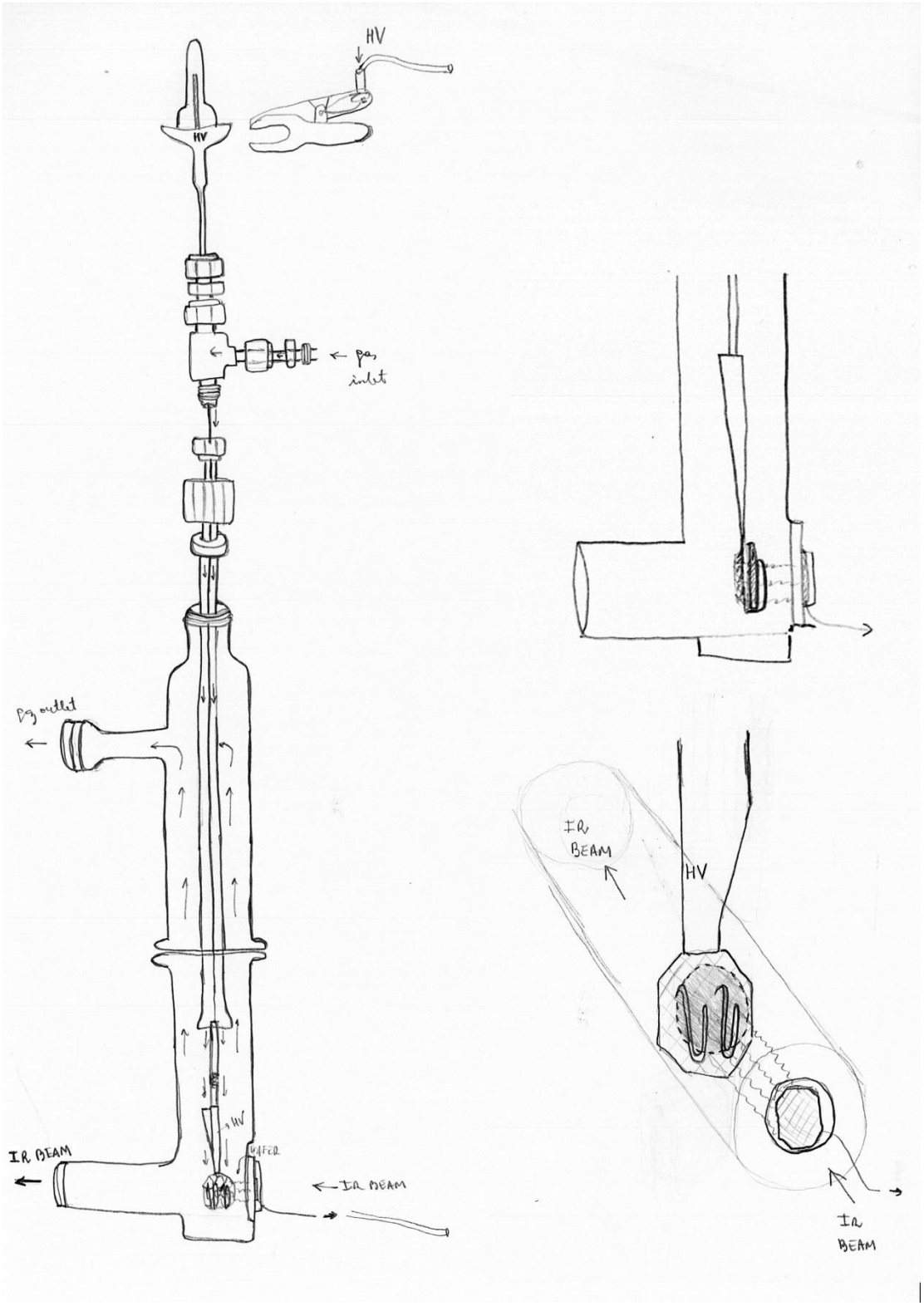

Figure S1: Scheme of the plasma *in-situ* DBD IR cell

Figure S2: Photograph of the *in-situ* DBD IR cell

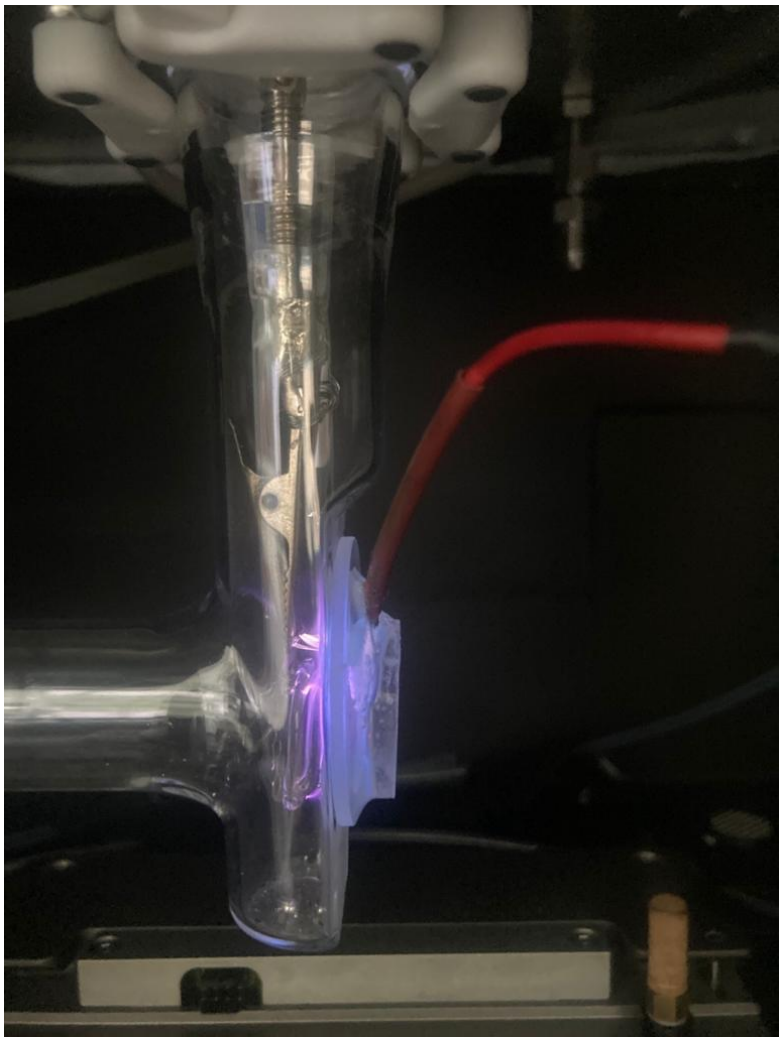

Figure S3: Photograph of the *in-situ* DBD IR cell with Ar plasma

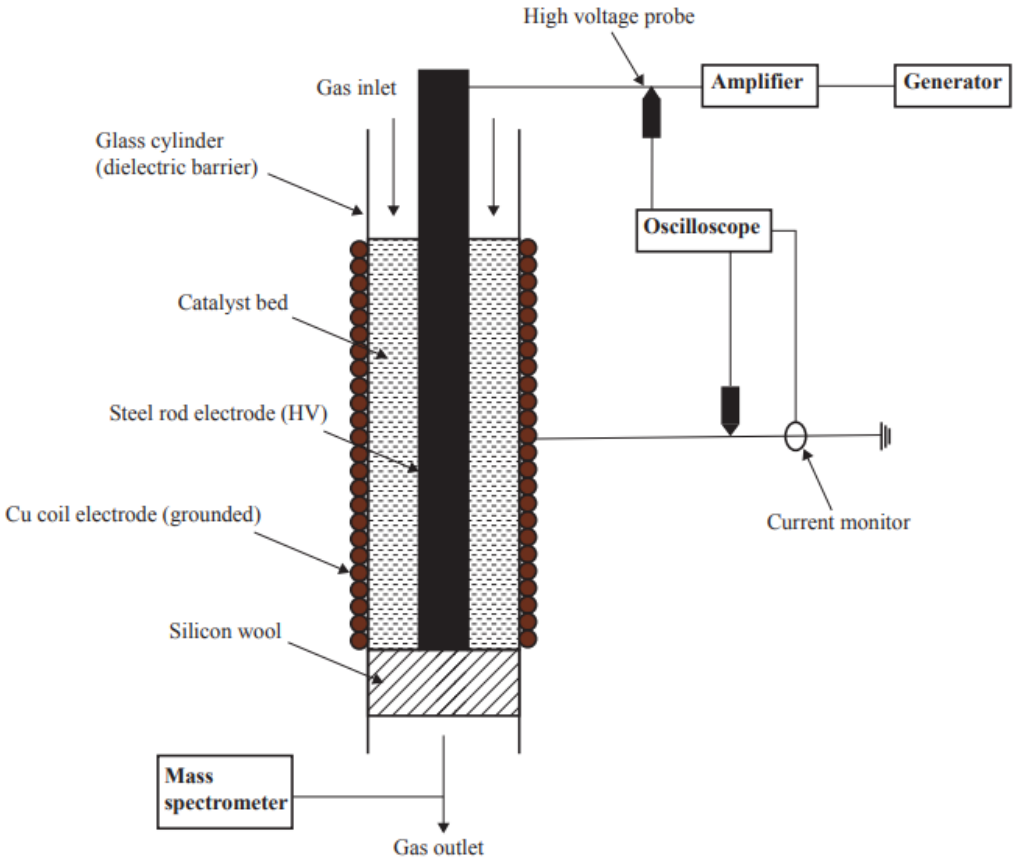

Figure S4: Schematic representation of the packed bed DBD reactor

S2. Formulas for the calculation of CO_2 and CH_4 conversion and CO, H_2 and C_2H_4 selectivity and yield

The MS data from the packed bed experiments was collected using PV MassSpec software and was exported for the calculation of CO_2 and CH_4 conversion (equation S1 and S2, respectively), CO selectivity (equation S3) and yield (equation S6), H_2 selectivity (equation S4) and yield (equation S7) and C_2H_4 selectivity (equation S5) and yield (equation S8). Note that the specific energy input (SEI), and thus the energy cost or energy efficiency of the reaction could not be calculated, as no capacitor was present in the electrical circuit and therefore no Lissajous plots were available for the calculation of the plasma power. However, this was not the focus of our study.

$$\chi_{CO_2}(\%) = \frac{\dot{n}_{CO_2,in} - \dot{n}_{CO_2,out}}{\dot{n}_{CO_2,in}} \cdot 100\ \% \qquad \text{(eq.S1)}$$

$$\chi_{CH_4}(\%) = \frac{\dot{n}_{CH_4,in} - \dot{n}_{CH_4,out}}{\dot{n}_{CH_4,in}} \cdot 100\ \% \qquad \text{(eq.S2)}$$

$$S_{\mathrm{C,CO}}(\%) = \frac{\dot{n}_{CO,out}}{(\dot{n}_{CH_4,in} - \dot{n}_{CH_4,out}) + (\dot{n}_{CO_2,in} - \dot{n}_{CO_2,out})} \cdot 100\ \% \qquad \text{(eq.S3)}$$

$$S_{H,H_2}(\%) = \frac{\dot{n}_{H_2,out}}{2 \cdot (\dot{n}_{CH_4,in} - \dot{n}_{CH_4,out})} \cdot 100\ \% \qquad \text{(eq.S4)}$$

$$S_{\mathrm{C},C_2H_4}(\%) = \frac{2 \cdot \dot{n}_{C_2H_4,out}}{(\dot{n}_{CH_4,in} - \dot{n}_{CH_4,out}) + (\dot{n}_{CO_2,in} - \dot{n}_{CO_2,out})} \cdot 100\ \% \qquad \text{(eq.S5)}$$

$$Y_{\mathrm{C,CO}}(\%) = \frac{\dot{n}_{CO,out}}{\dot{n}_{CO_2,in} + \dot{n}_{CH_4,in}} \cdot 100\ \% \qquad \text{(eq.S6)}$$

$$Y_{H,H_2}(\%) = \frac{\dot{n}_{H_2,out}}{2 \cdot \dot{n}_{CH_4,in}} \cdot 100\ \% \qquad \text{(eq.S7)}$$

$$Y_{\mathrm{C},C_2H_4}(\%) = \frac{2 \cdot \dot{n}_{C_2H_4,out}}{\dot{n}_{CO_2,in} + \dot{n}_{CH_4,in}} \cdot 100\ \% \qquad \text{(eq.S8)}$$

With $\dot{n}_i$ the molar flow rate of species i.

S3. DBD packed bed experiments: calibration curves

In this section, the calibration curves used for calculation of CO_2 and CH_4 conversion and CO, H_2 and C_2H_4 selectivity and yield, using the formulas given in section S2, are given. The C_2H_4 concentration was calibrated using FTIR, while the CO_2, H_2, CO and CH_4 concentrations were calibrated using MS. In order to account for the contribution of CO_2 to the m/z = 28 signal, to avoid an underestimation of CO production, CO_2 was also calibrated using the m/z = 28 signal (see Figure S10).

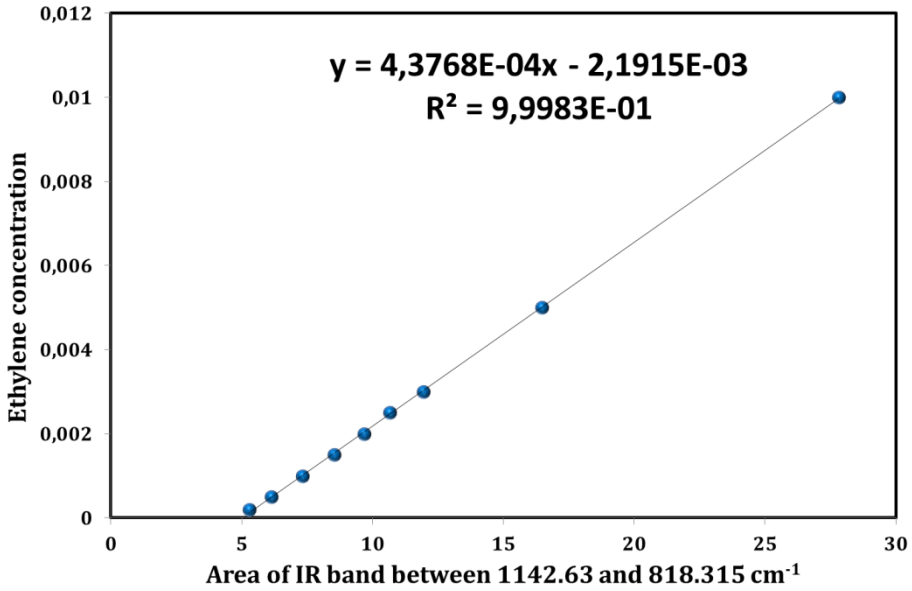

Figure S5: Ethylene calibration curve by FTIR

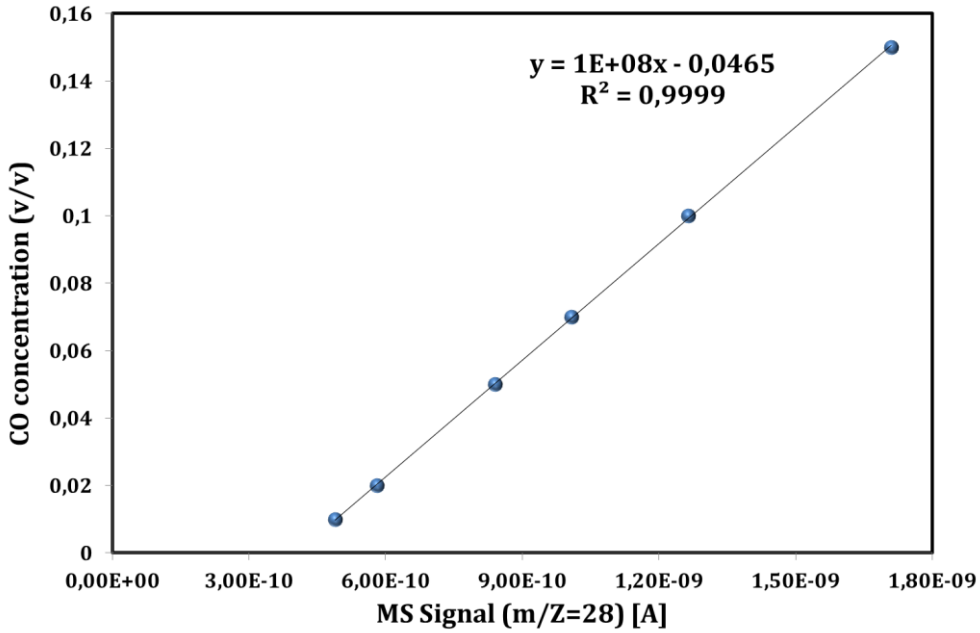

Figure S6: CO calibration curve by MS

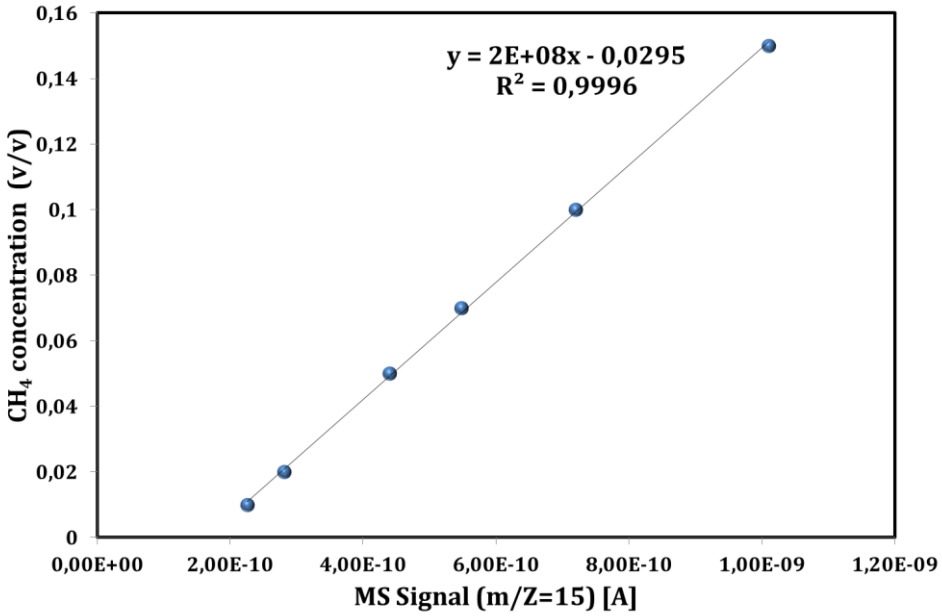

Figure S7: CH_4 calibration curve by MS

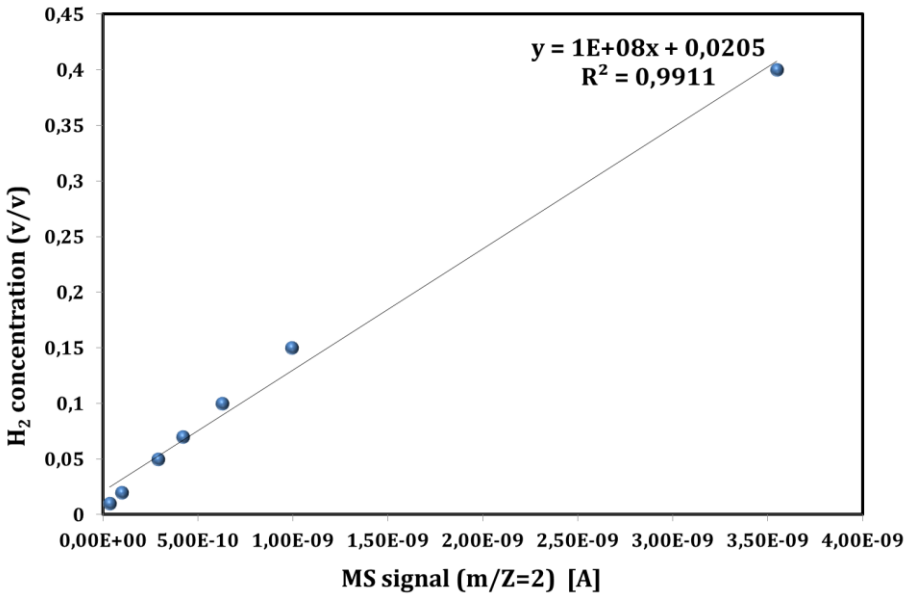

Figure S8: H_2 calibration curve by MS

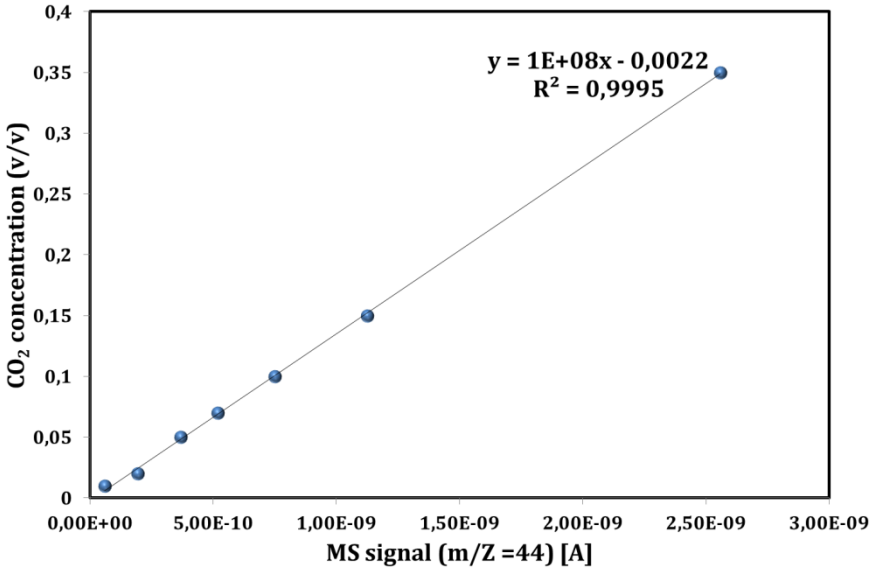

Figure S9: CO_2 calibration curve by MS

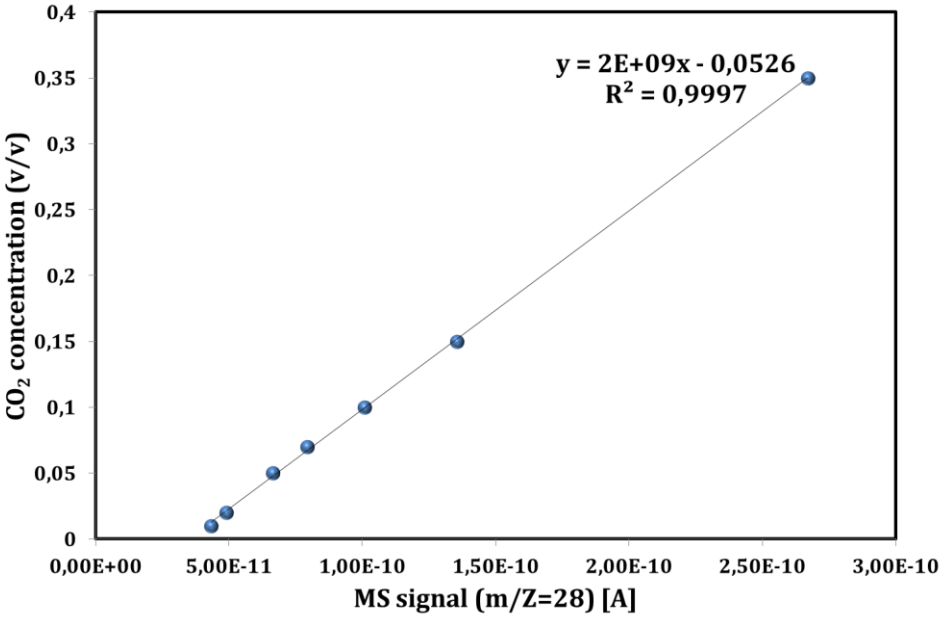

Figure S10: Contribution of CO_2 on the m/Z=28 MS signal

S4. Catalyst characterization

S4.1 H_2-TPR

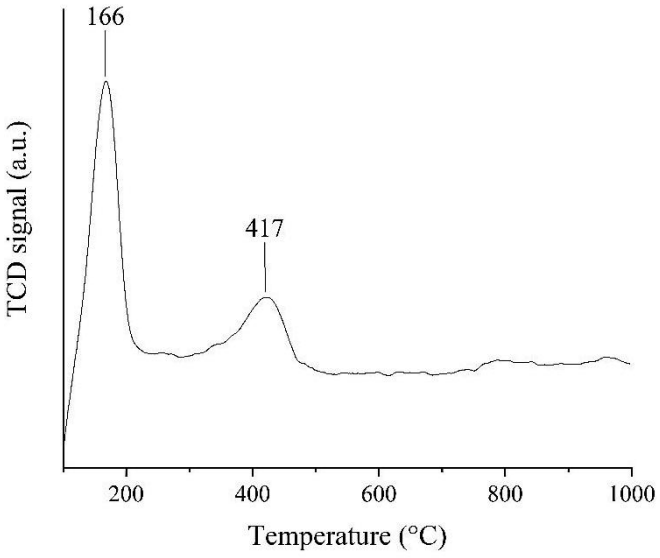

Figure S11: H_2-TPR profile of 3 wt% Ru/SiO_2

S4.2 X-ray diffraction

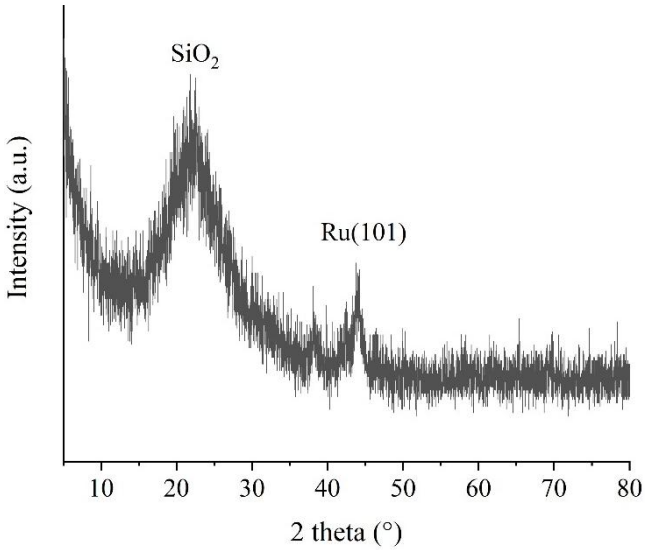

Figure S12: XRD diffractogram of 3 wt% Ru/SiO_2

S4.3 N_2-sorption

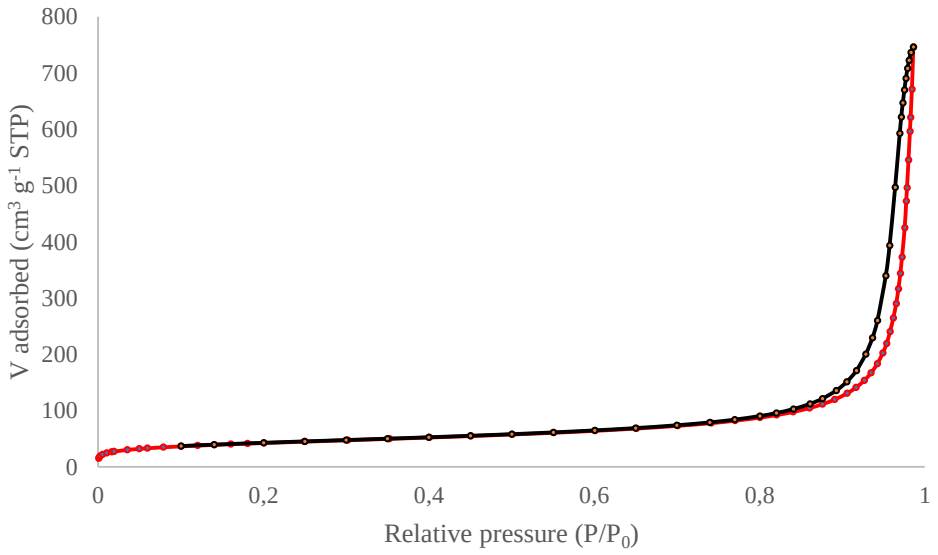

Figure S13: N_2-sorption isotherm of the SiO_2 support, showing adsorption in red and desorption in black

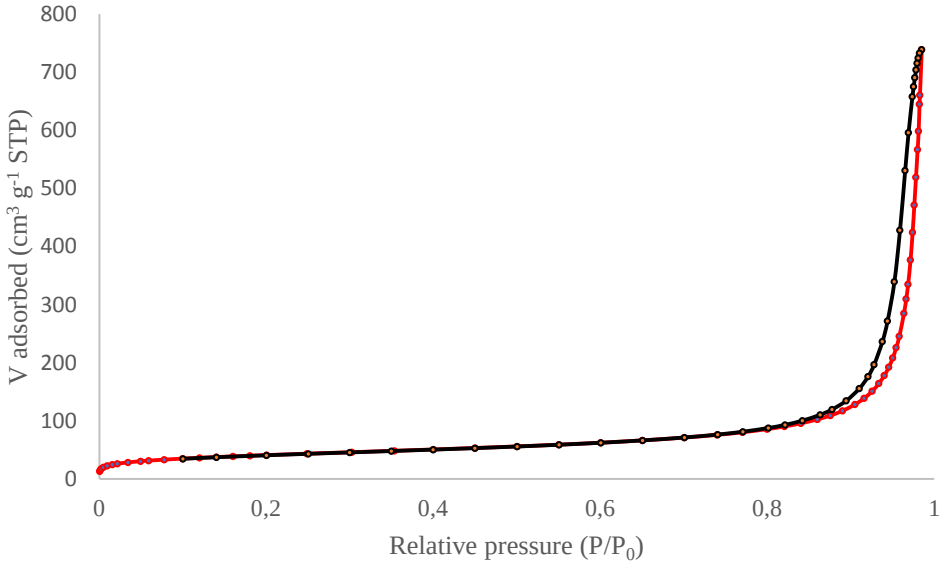

Figure S14: N_2-sorption isotherm of the 3 wt% Ru/SiO_2 sample, showing adsorption in red and desorption in black

S4.4 EDS-SEM

Energy-dispersive X-ray spectroscopy (EDS) coupled to SEM was used for the elemental analysis of Ru/SiO_2 catalyst using an EDAX XM2-30T apparatus. Two separate regions of the catalyst were analyzed. The elemental analysis verified the presence of Na, Al, Si, O and Ru, as shown in Figure S15, with the presence of Al and Na possibly being due to impurities in the SiO_2 support. The carbon is due to the sample holder. The quantification of the main elements is shown in Table S1. The amount of Ru found with this semi-quantitative technique was 4.64 and 5.44 wt% for the region 1 and 2, respectively. These values are both higher than the expected one (3wt%Ru), possibly due to the presence of Ru clusters and the quantitative limitation of this technique.

Elemental mapping is shown in Figure S16 and the linear EDS analysis of a Ru cluster is presented in Figure S17.

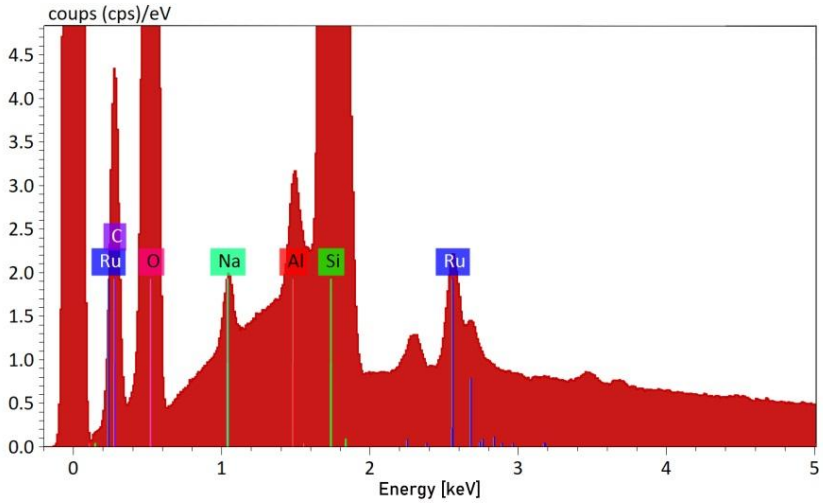

Figure S15: Energy-dispersive X-ray spectroscopy of the Ru/SiO_2 catalyst

Table S1: Quantification of the elemental analysis of Ru/SiO_2 by EDS in the two measured regions

Element	Region 1		Region 2	
	% mass.	% atom.	% mass.	% atom.
Na	0.78	0.99	1.47	1.87
Al	1.03	1.11	1.15	1.24
Si	93.55	96.57	91.93	95.32
Ru	**4.64**	**1.33**	**5.44**	**1.57**

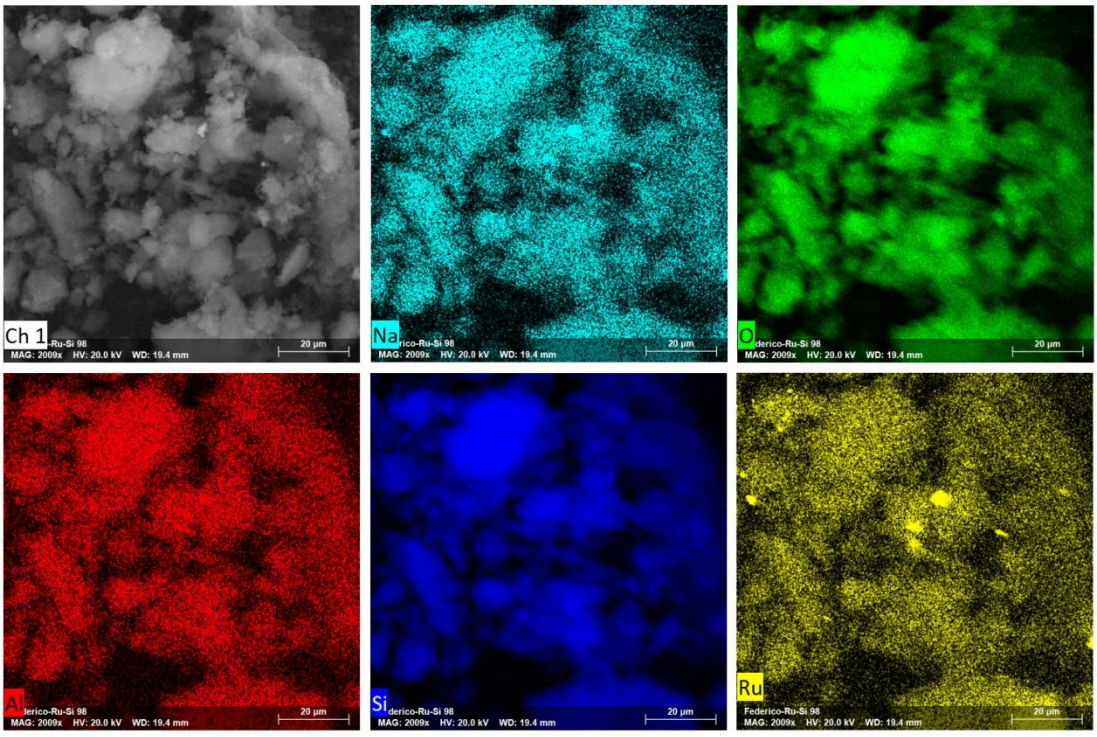

Figure S16: EDS elemental mapping of the Ru/SiO_2 catalyst showing the mapping of Na, O, Al, Si and Ru

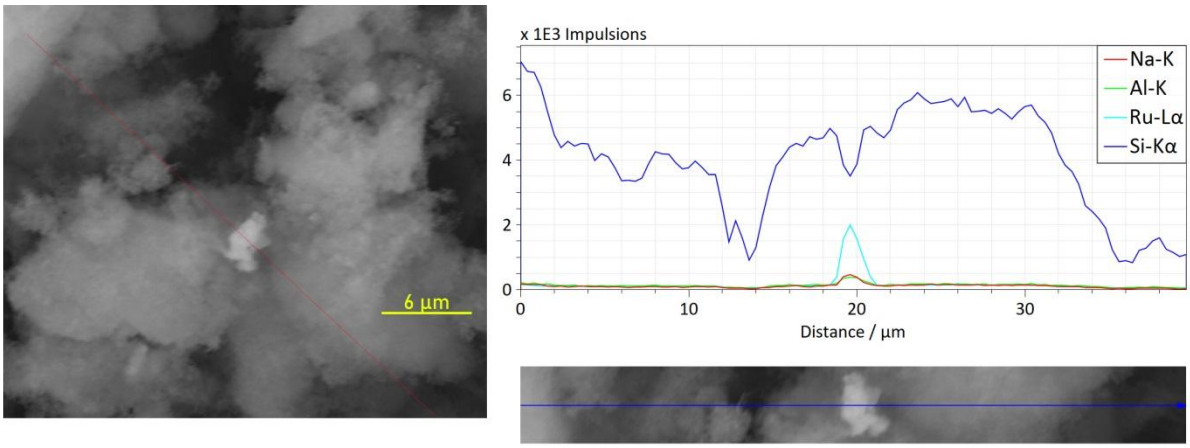

Figure S17: Linear EDS analysis of Ru cluster

S5. *In-situ* FTIR in plasma

S5.1 SiO_2 support

In order to disentangle the effects of the individual reactants in DRM (i.e. CO_2 and CH_4), we performed experiments with CO_2/Ar and CH_4/Ar plasma in addition to experiments with a mixture of the reactants. The experimental procedures are slightly different from the procedures used for DRM, and are discussed, along with presenting the experimental results, in section S5.1.1. and section S5.1.2., for CO_2/Ar and CH_4/Ar, respectively.

S5.1.1. CO_2/Ar

First, the SiO_2 wafer was introduced into the cell and the catalyst was activated at 350 °C for 3 h under secondary vacuum (10^{-7} Torr). Then, the SiO_2 sample was exposed to a mixture of 7 mL min^{-1} (STP) CO_2 and 13 mL min^{-1} (STP) Ar to monitor CO_2 adsorption on the SiO_2 support before ignition of the plasma. Subsequently, the plasma was ignited at a voltage of ~ 30 kV and a frequency of 3 kHz. Upon stabilization of the spectra, the plasma was extinguished.

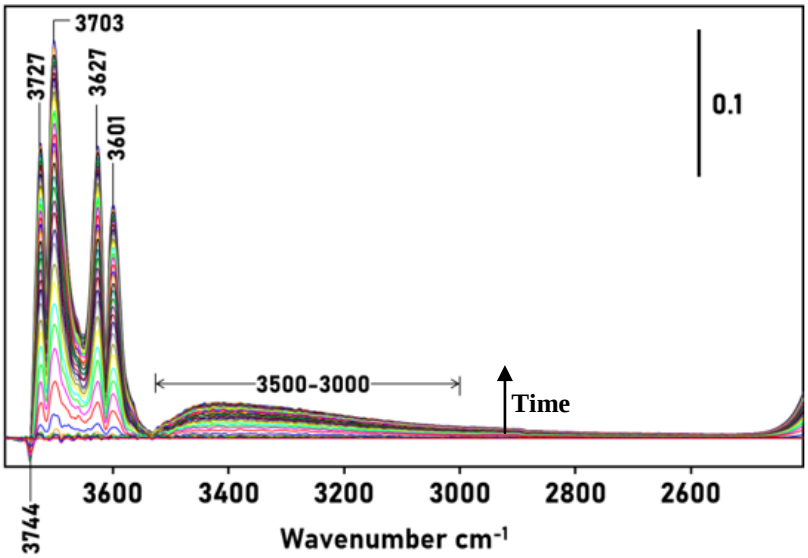

Figure S18: FTIR difference spectra of the SiO_2 support exposed to CO_2/Ar before plasma ignition in the 3800-2400 cm^{-1} region as a function of time

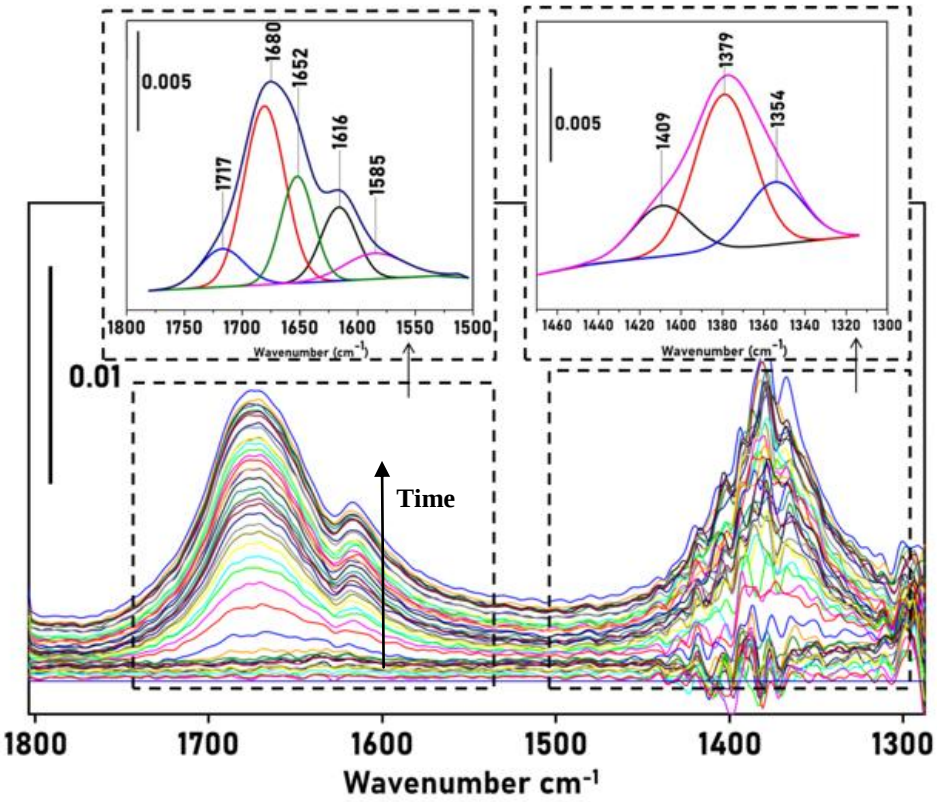

Figure S19: FTIR difference spectra of the SiO_2 support exposed to CO_2/Ar before plasma ignition in the 1800-1300 cm^{-1} region as a function of time with details of the 1800-1500 and 1480-1300 cm^{-1} regions

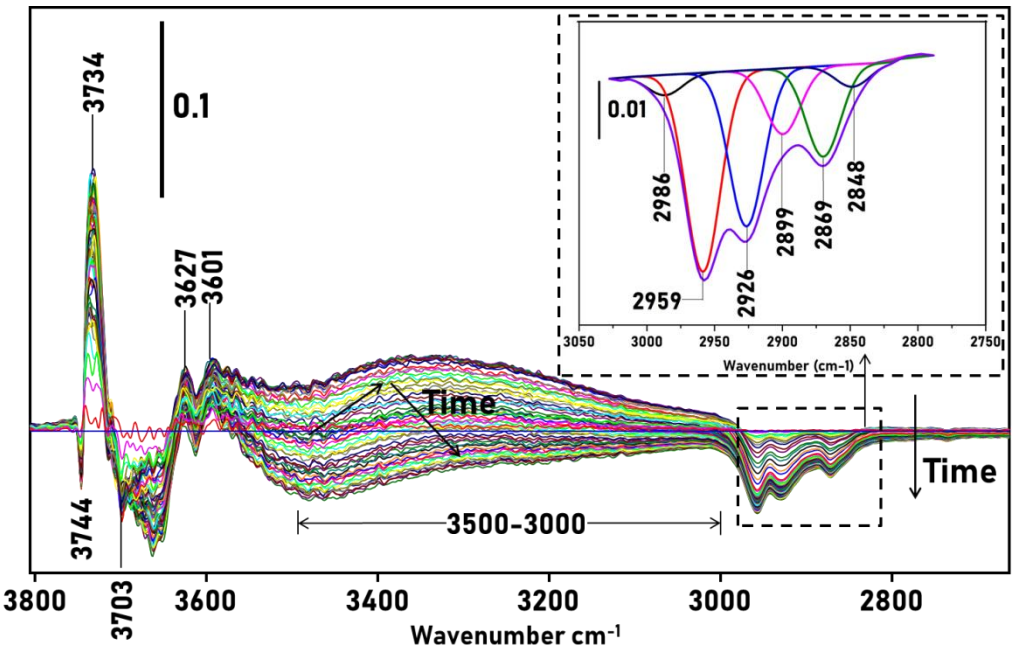

Figure S20: FTIR difference spectra of the SiO_2 support exposed to CO_2/Ar plasma in the 3800-2600 cm^{-1} region as a function of time with detail of the 3050-2750 cm^{-1} region

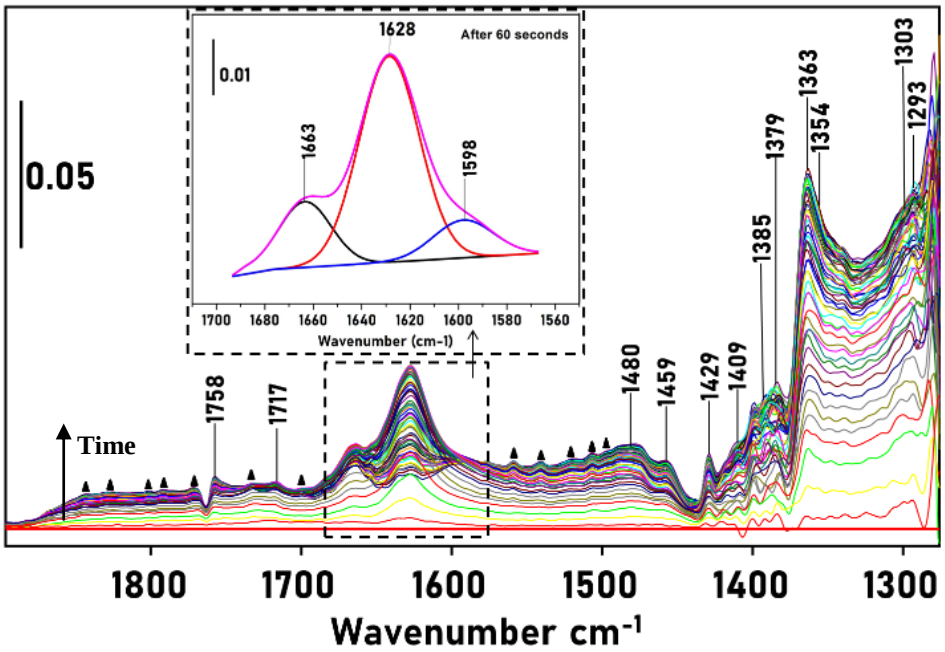

Figure S21: FTIR difference spectra of the SiO_2 support exposed to a CO_2/Ar plasma in the 1900-1275 cm^{-1} region as a function of time with detail of the 1710-1550 cm^{-1} region; (▲) indicates bands corresponding to H_2O vapor

S5.1.2. CH_4/Ar

The procedure described in section S5.1.1 was again used for the SiO_2 support, with a gas composition of 7 mL min^{-1} (STP) CH_4 and 13 mL min^{-1} (STP) Ar.

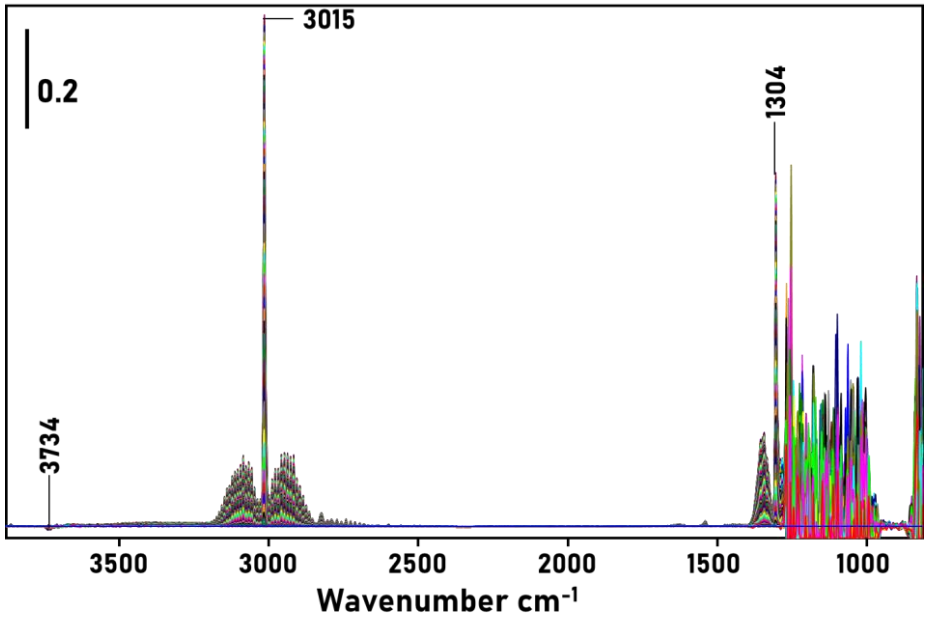

Figure S22: FTIR difference spectra of the SiO_2 support exposed to CH_4/Ar before plasma ignition in the 3900-800 cm^{-1} region as a function of time

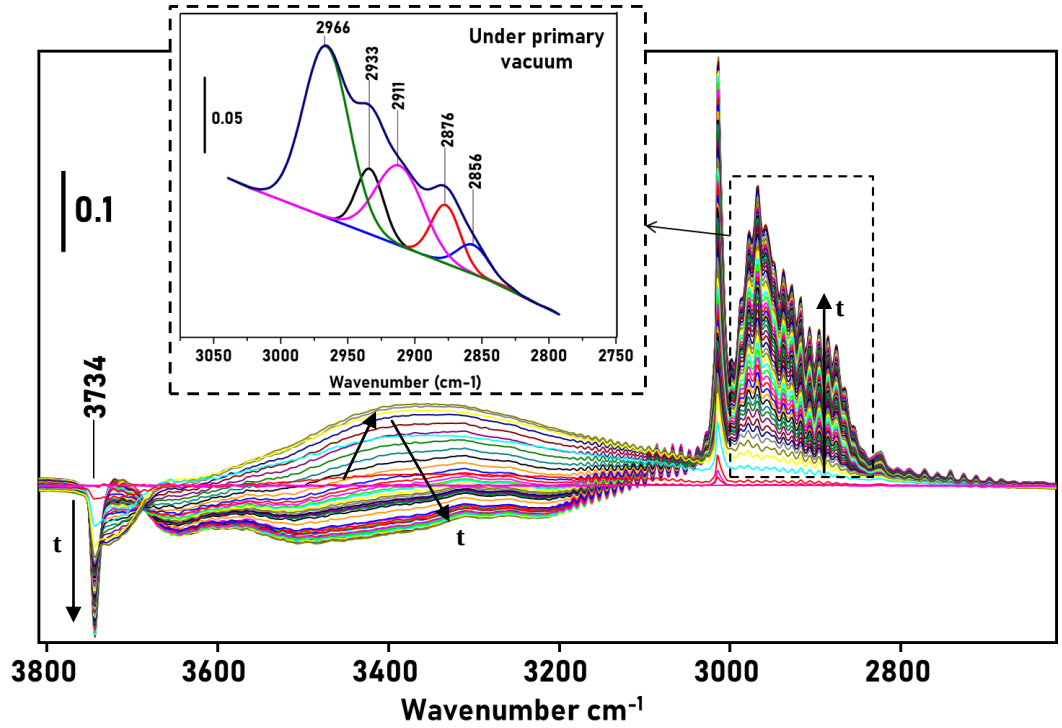

Figure S23: FTIR difference spectra of the SiO_2 support exposed to a CH_4/Ar plasma in the 3800-2600 cm^{-1} region as a function of time with detail of the 3075-2750 cm^{-1} region under primary vacuum

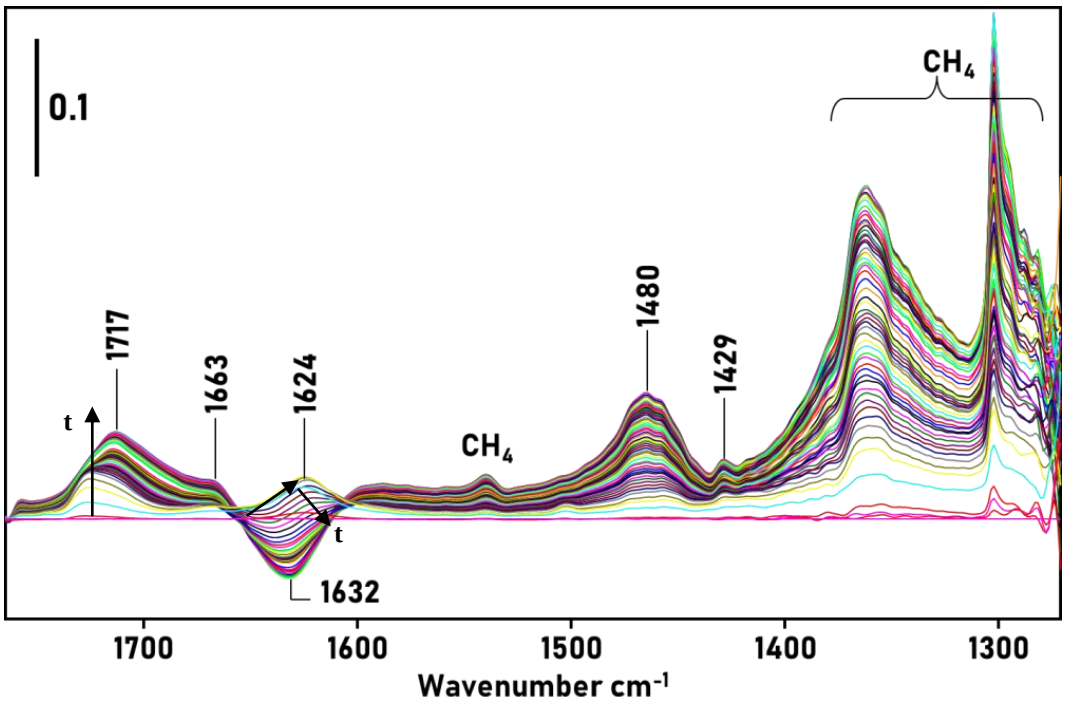

Figure S24: FTIR difference spectra of the SiO_2 support exposed to a CH_4/Ar plasma in the 1760-1275 cm^{-1} region as a function of time

S5.1.3. Dry reforming of methane (DRM)

For the DRM experiments, the procedure as described in section 2.2.2 in the main paper was used. Below, relevant results which are referenced in the main paper, and complementary to the results presented there, are shown.

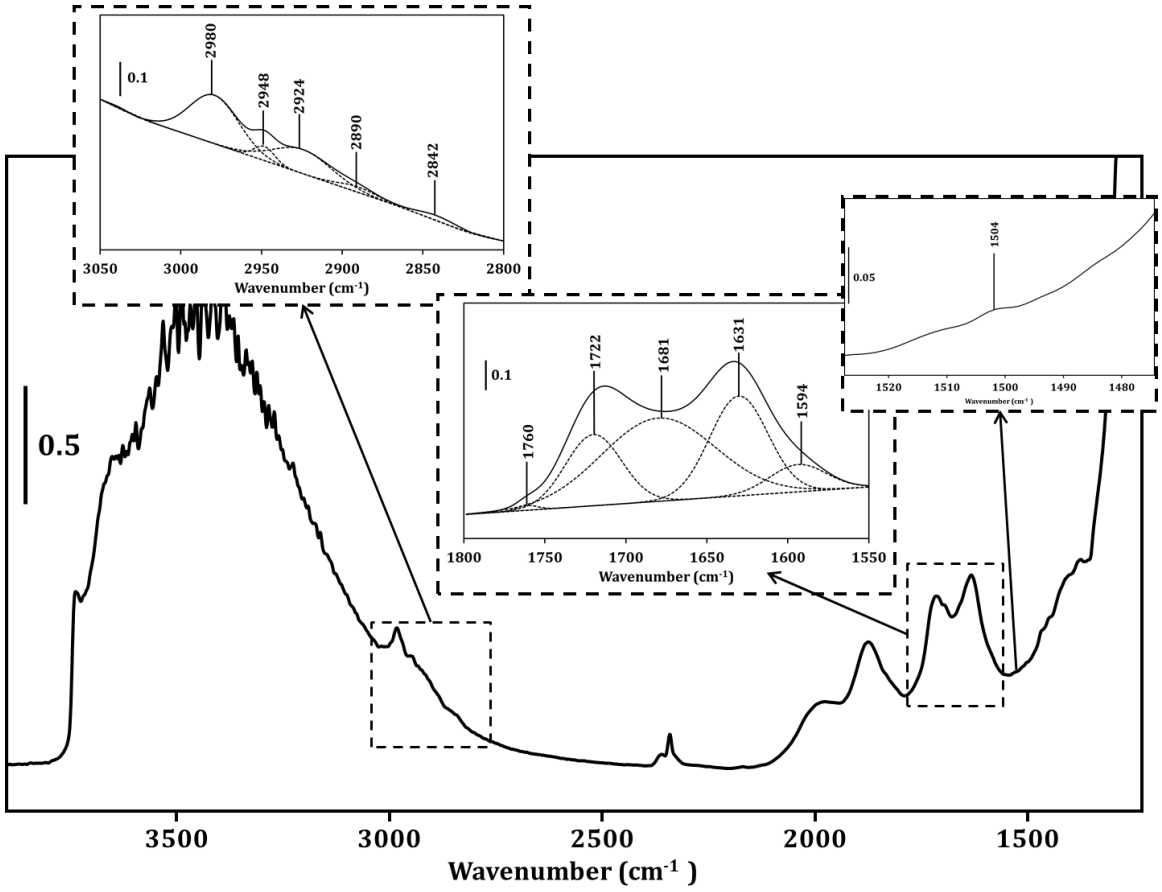

Figure S25: FTIR difference spectra of the SiO_2 support under secondary vacuum after exposure to $CO_2/CH_4/Ar$ plasma in the 4000-1250 cm^{-1} region

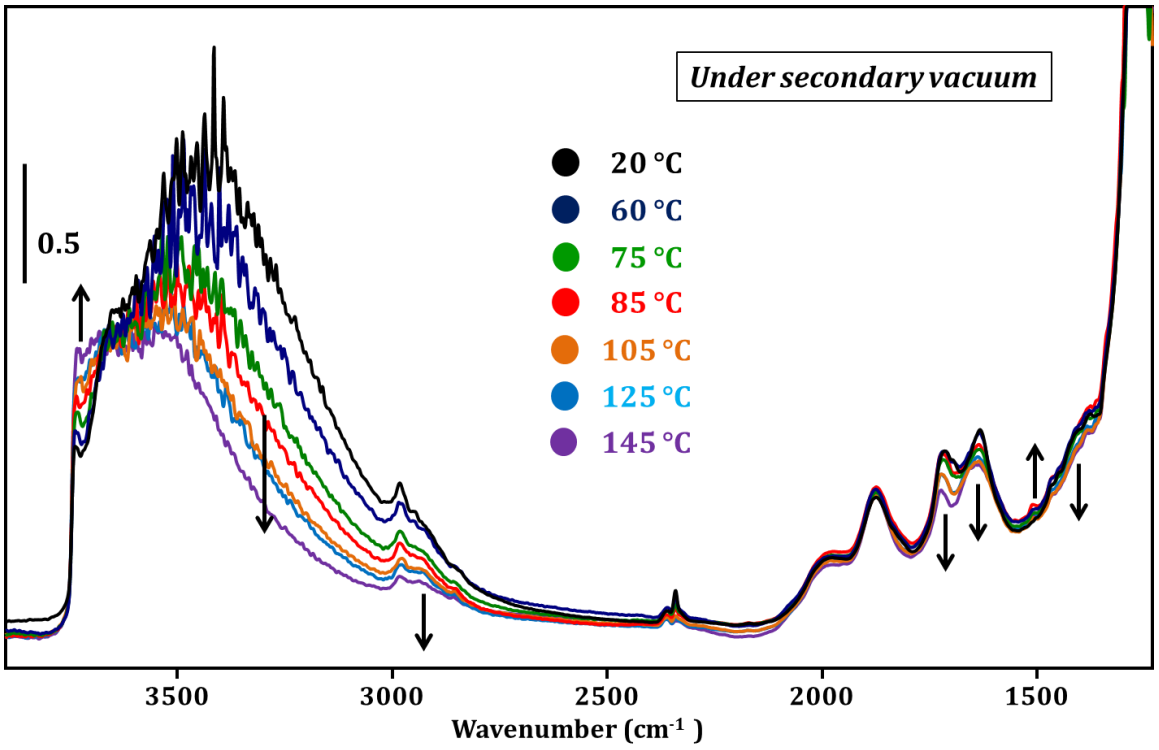

Figure S26: FTIR difference spectra of the SiO_2 support after exposure to $CO_2/CH_4/Ar$ plasma under secondary vacuum exposed to increasing temperatures (20 – 145 °C) in the 4000-1250 cm^{-1} region

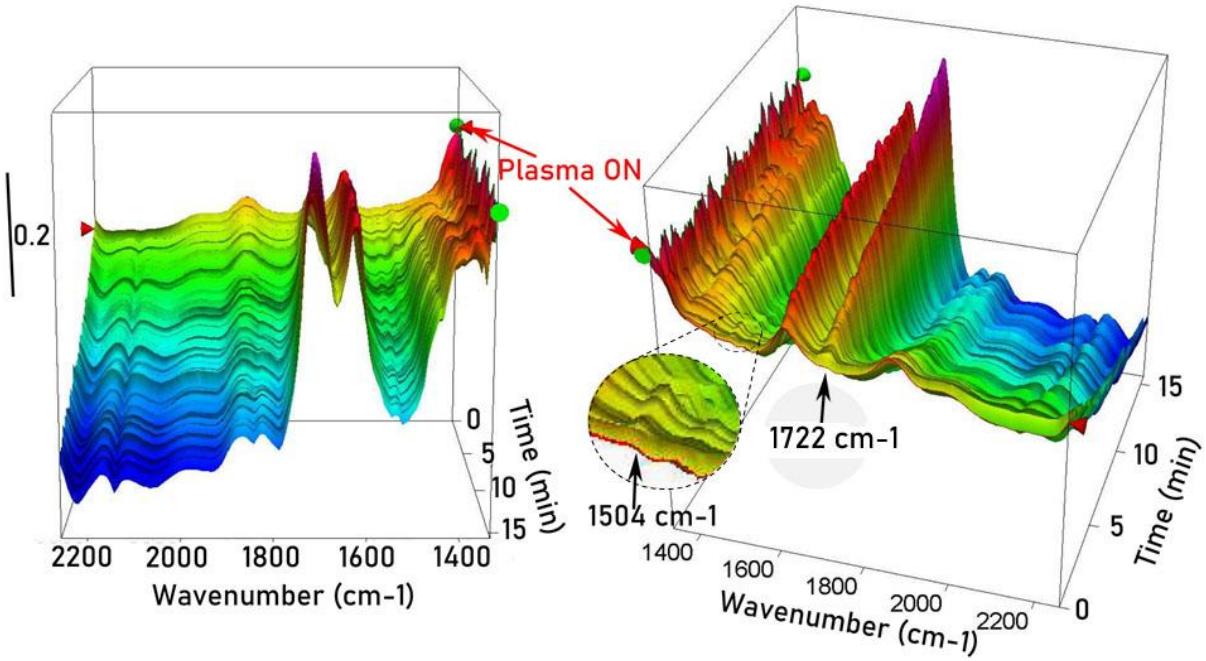

Figure S27: FTIR difference spectra of the SiO_2 support during DRM in plasma in the 1900-1300 cm^{-1} region as a function of time

S5.2. Ru/SiO_2 catalyst

In contrast to the SiO_2 support alone, the Ru-loaded SiO_2 catalyst was reduced *in-situ* using H_2/Ar plasma. Section S5.2.1. contains the spectra recorded during the *in-situ* reduction that preceded the DRM experiment, as referenced in the main paper.

Again, in order to disentangle the effects of the individual reactants of DRM (i.e. CO_2 and CH_4), we performed experiments with CO_2/Ar and CH_4/Ar plasma in addition to experiments with a mixture of the reactants. The experimental procedures are slightly different from the procedures used for DRM, and are discussed, along with presenting the results, in section S5.2.2. and section S5.2.3. for CO_2/Ar and CH_4/Ar, respectively.

S5.2.1. H_2/Ar

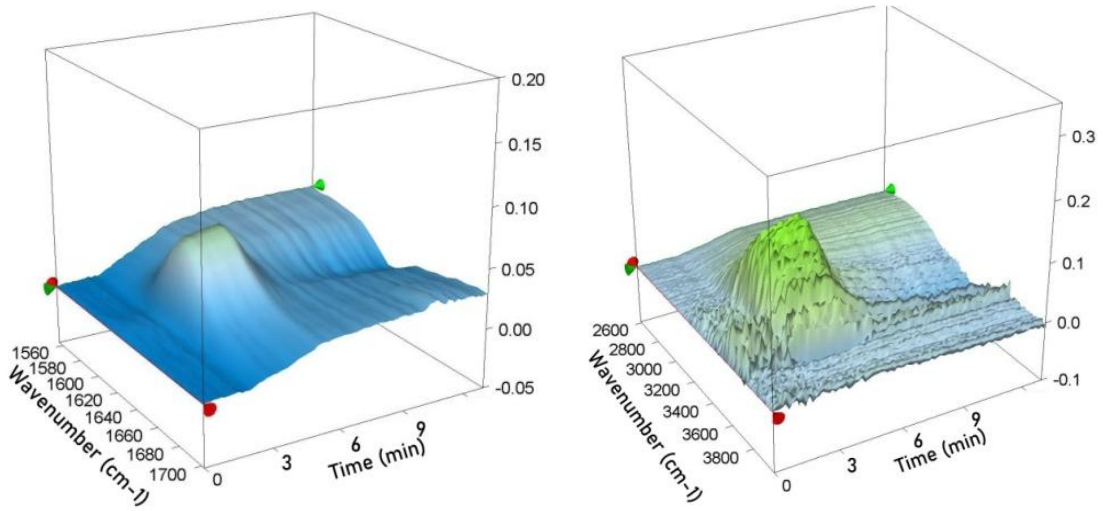

Figure S28: FTIR spectra in the 1700-1560 (left) and 3900-2600 cm^{-1} (right) region as a function of time recorded during the *in-situ* reduction of the Ru/SiO_2 catalyst by H_2/Ar plasma

S5.2.2. CO_2/Ar

The procedure described in section S5.1.1 was again used for the Ru/SiO_2 catalyst, with the addition of an *in-situ* reduction using H_2/Ar plasma (20 vol% H2 and 80 vol% Ar, with a total gas flow rate of 20 mL min^{-1} (STP)) at ~ 28 kV for 20 min right after the catalyst activation under vacuum. This reduction was followed by purging the cell under vacuum (0.3 Torr) to remove the water formed during the reduction step, and remove remaining H_2 in the cell.

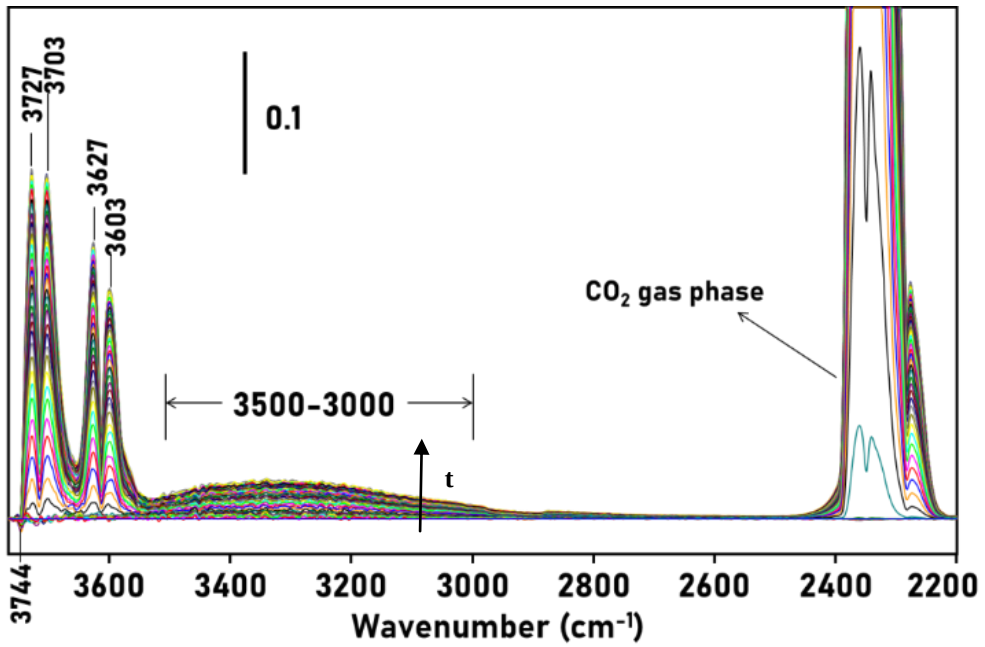

Figure S29: FTIR difference spectra of the 3 wt% Ru/SiO_2 catalyst exposed to CO_2/Ar before plasma ignition in the 3800-2200 cm^{-1} region as a function of time

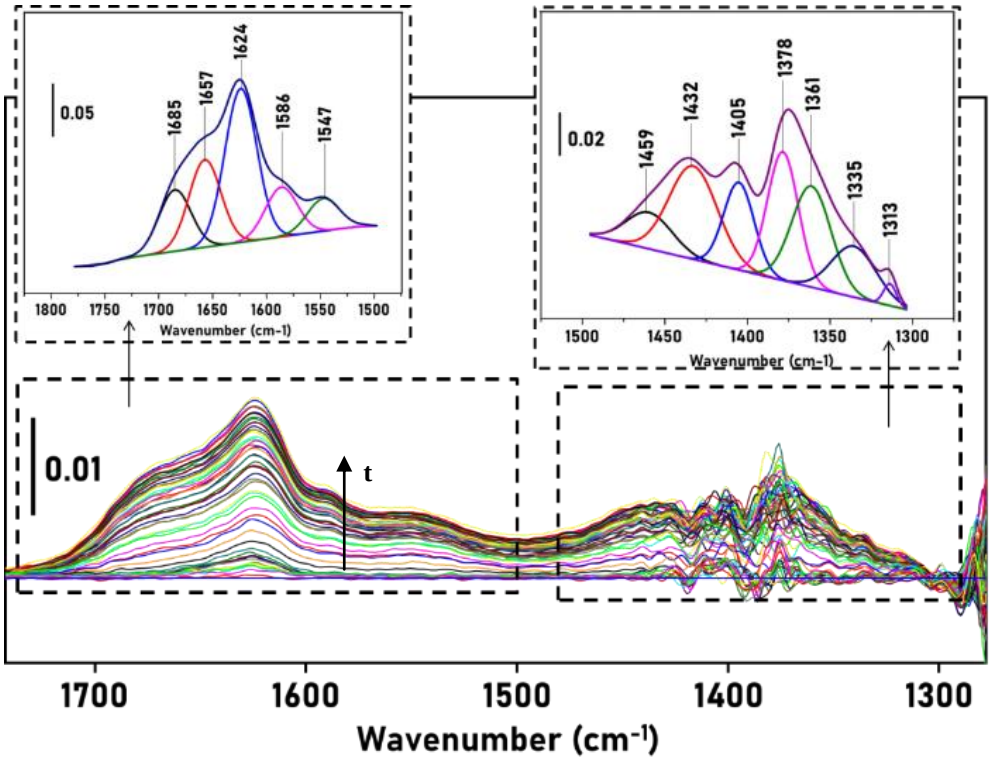

Figure S30: FTIR difference spectra of the 3wt% Ru/SiO_2 catalyst exposed to CO_2/Ar before plasma ignition in the 1750-1275 cm^{-1} region as a function of time with details of the 1750-1475 and 1525-1300 cm^{-1} regions

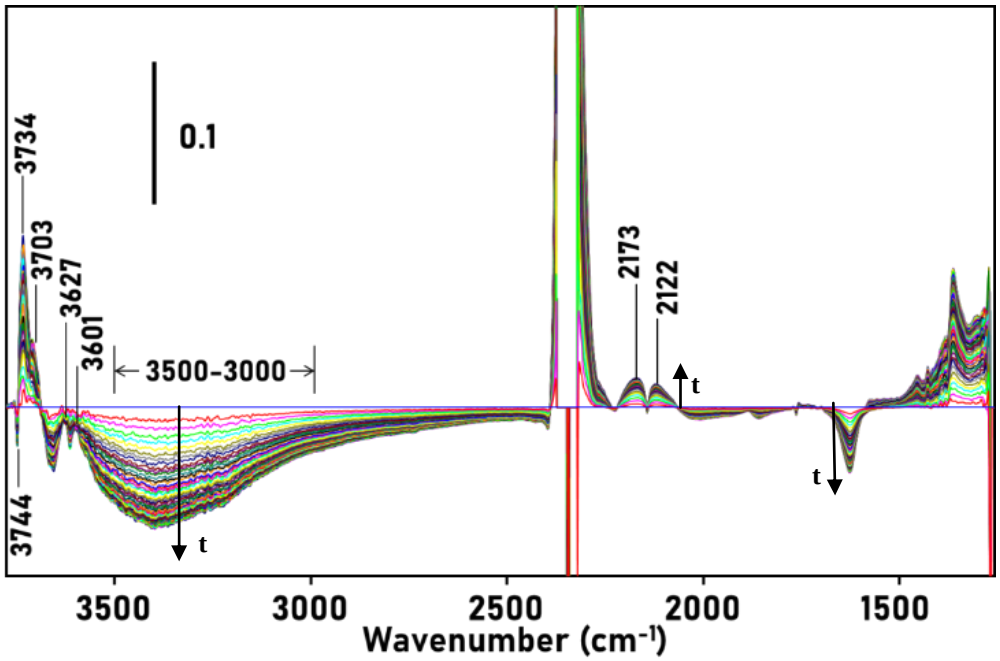

Figure S31: FTIR difference spectra of the 3wt% Ru/SiO_2 catalyst exposed to CO_2/Ar plasma in the 3750-2600 cm^{-1} region as a function of time

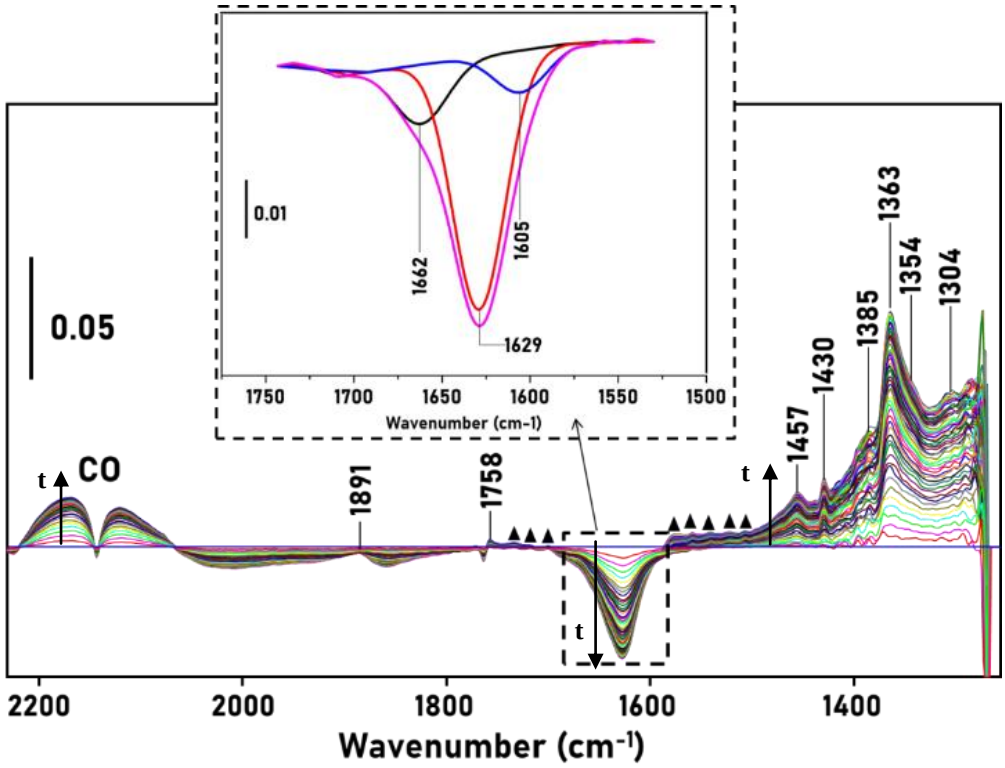

Figure S32: FTIR difference spectra of the SiO_2 support exposed to a CO_2/Ar plasma in the 2220-1250 cm^{-1} region as a function of time with detail of the 1750-1525 cm^{-1} region at steady state; (▲) indicates bands corresponding to H_2O vapor

S5.2.3. CH_4/Ar

The procedure described in section S5.2.2 was again used, with a gas composition of 7 mL min^{-1} (STP) CH_4 and 13 mL min^{-1} (STP) Ar.

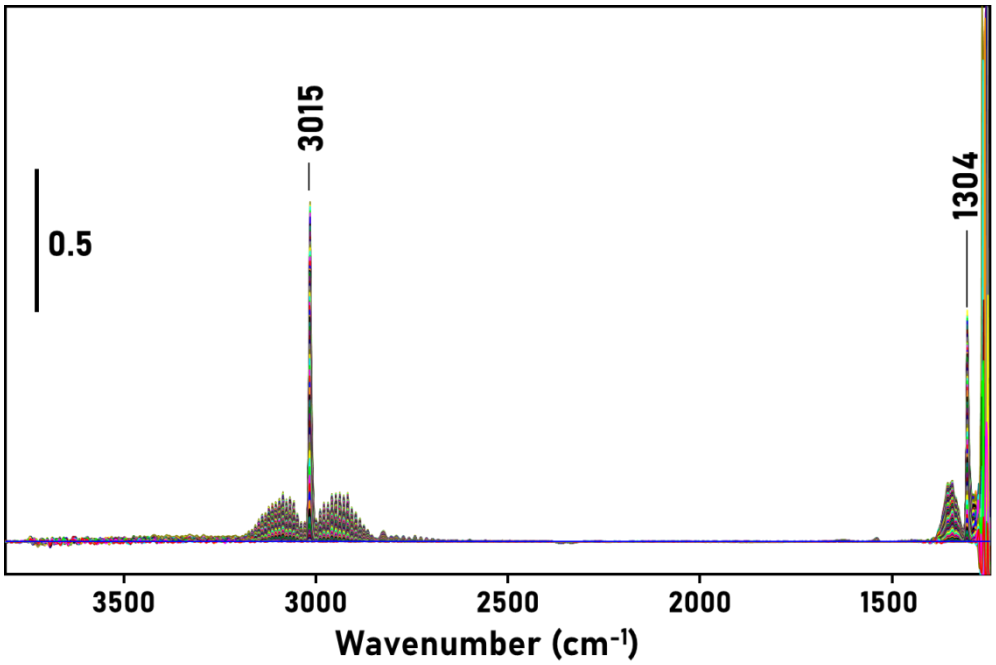

Figure S33: FTIR difference spectra of the 3wt% Ru/SiO_2 catalyst exposed to CH_4/Ar before plasma ignition in the 3900-1250 cm^{-1} region as a function of time

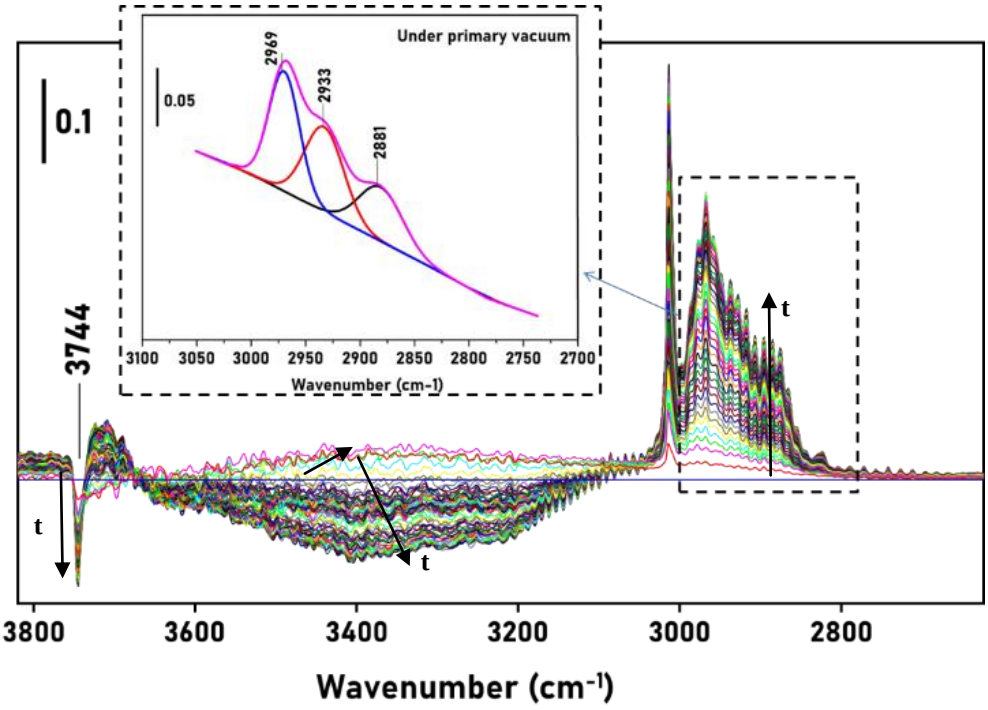

Figure S34: FTIR difference spectra of the 3wt% Ru/SiO_2 catalyst exposed to a CH_4/Ar plasma in the 3800-2600 cm^{-1} region as a function of time with detail of the 3075-2750 cm^{-1} region under primary vacuum

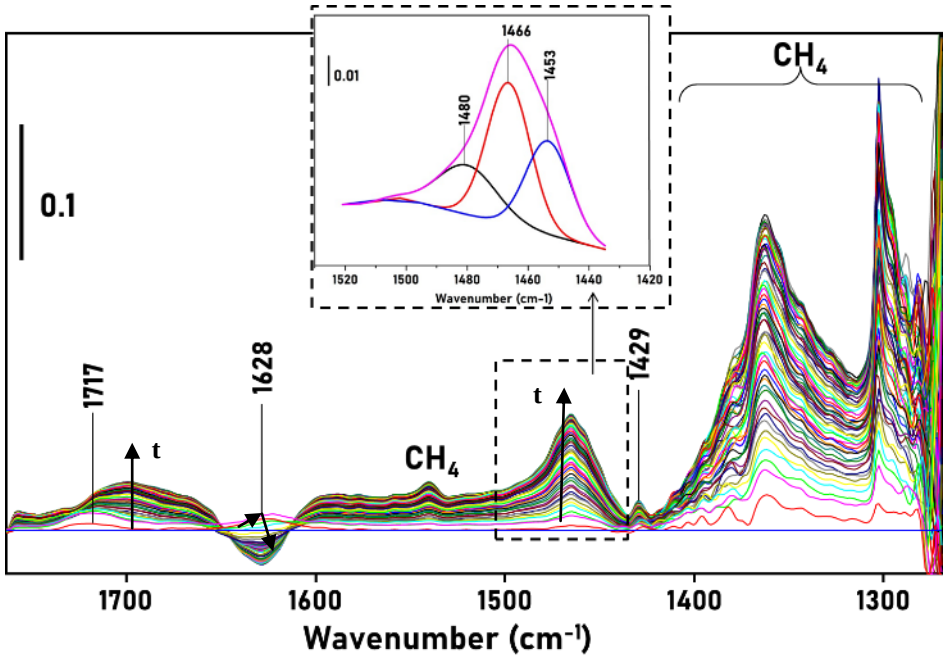

Figure S35: FTIR difference spectra of the 3wt% Ru/SiO_2 catalyst exposed to a CH_4/Ar plasma in the 1775-1275 cm^{-1} region as a function of time with detail of the 1520-1435 cm^{-1} region

S5.2.4. Dry reforming of methane (DRM)

Again, for the DRM experiments, the procedure as described in section 2.2.2 in the main paper was used. Below, relevant results which are referenced in the main paper, and complementary to the results presented there, are shown.

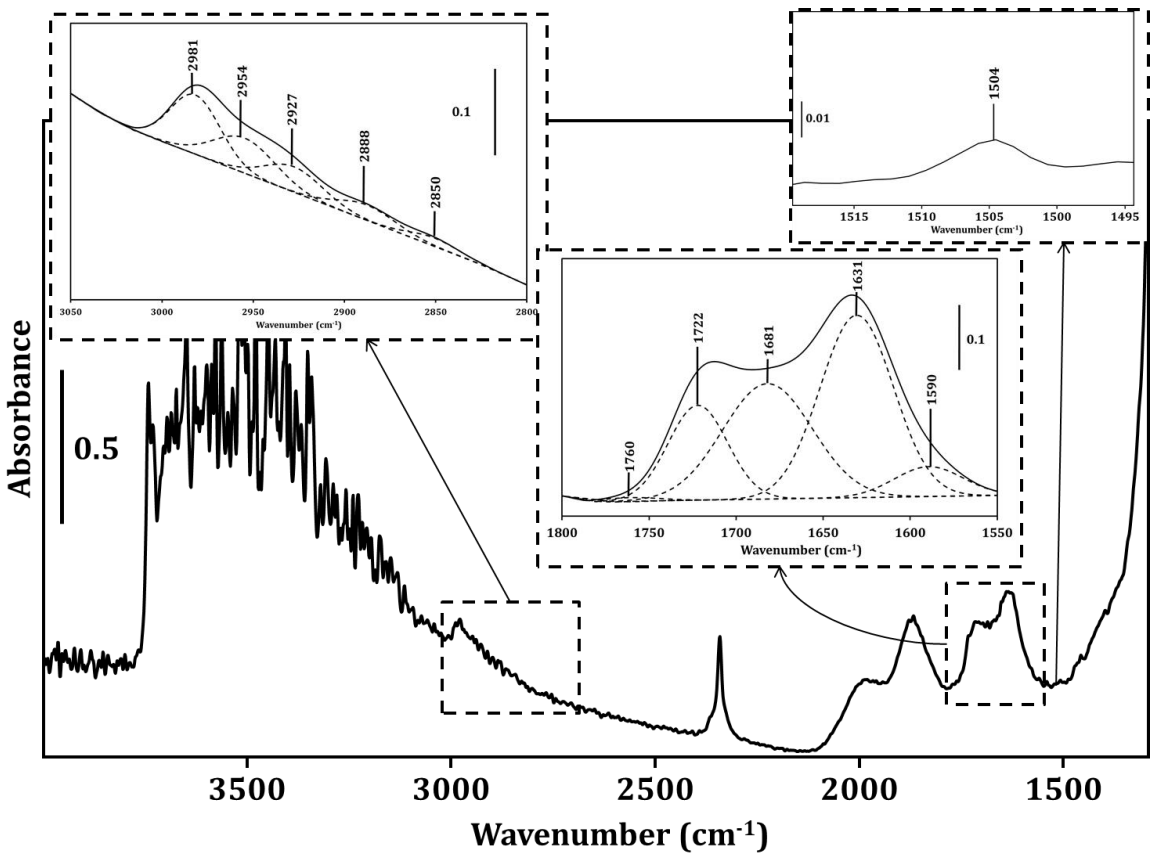

Figure S36: FTIR spectrum (4000-1300 cm^{-1}) at steady state of the 3wt% Ru/SiO_2 catalyst under vacuum after exposure to $CO_2/CH_4/Ar$ plasma

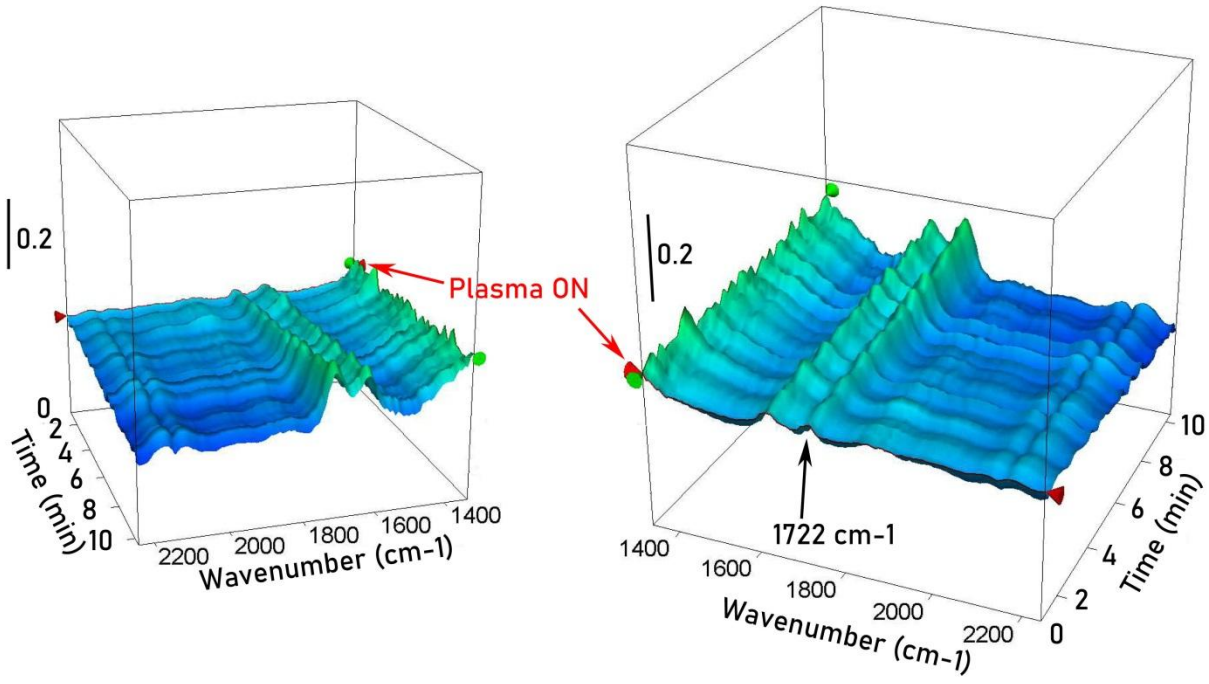

Figure S37: FTIR difference spectra of the 3wt% Ru/SiO_2 catalyst during DRM in plasma in the 2200-1400 cm^{-1} region as a function of time

S5.3. Activity measurements in the *in-situ* cell

Below, we show the activity measurements during plasma-assisted DRM over SiO_2 and Ru/SiO_2 in our novel *in-situ* cell (see Table S2). Clearly, while in principle we work under *operando* conditions, as activity can be measured in parallel to our FTIR measurements, the observed conversion of both CO_2 and CH_4 is low, so that we are forced to proceed with activity testing in a different reactor setup, namely a packed bed DBD reactor.

		SiO_2 wafer	3wt%Ru/SiO_2 wafer
CO_2 conversion (%)		0.52 ± 0.05	0.5 ± 0.1
CH_4 conversion (%)		0.73 ± 0.05	0.75 ± 0.05
H_2	Yield (%)	0.66	0.44
	Selectivity (%)	91 ± 2	59 ± 2
CO	Yield (%)	0.56	0.32
	Selectivity (%)	90 ± 2	50 ± 9
C_2H_4 (ethylene)	Yield (%)	undetectable	undetectable
	Selectivity (%)	undetectable	undetectable

S6. Thermal *in-situ operando* IR "sandwich" cell

To distinguish the effect of plasma-induced heating from other plasma effects, the Ru/SiO_2 wafer was also tested in a thermal *in-situ operando* IR "sandwich" cell at 100 and 150 °C (i.e. around the observed temperature range of the catalyst wafer in the plasma, as described in section 3.2.3 of the main paper). More information on the setup and experimental procedure is available below, in addition to the experimental results, which are given in section S6.1. and referenced in the main paper in section 3.2.3.

A schematic representation of the thermal *in-situ operando* (or "sandwich" cell **[1]**) is given in figure S38. The H_2, CH_4, CO_2 and Ar gas inlet is controlled by four separate Brooks Delta Smart II flow meters, which are operated through a corresponding in-house computer program. The gas inflow is mixed and then introduced directly onto the catalyst wafer via the sample holder, whereas the gas outlet is placed on the opposite side of the sample holder. Additionally, a thermocouple is placed in the sample holder, close to the catalyst wafer, in order to monitor the temperature inside the cell. The sample holder is positioned inside an oven to allow for heating of the catalyst wafer. The *sandwich* cell is positioned inside the sample compartment of a Thermo Fisher scientific Nicolet 6700 spectrometer with a liquid nitrogen cooled mercury-cadmium-telluride (MCT) detector. The sample holder is sealed with four (two on each side) KBr windows for the IR beam to pass through, ensuring an IR transmission window in the 4000-400 cm^{-1} range. The catalyst is introduced as a self-supported wafer in the sample holder.

First, the reduced self-supported 3 wt% Ru/SiO_2 wafer was put into the sample holder. Then, the sample holder was introduced into the cell and the catalyst was reduced *in-situ* at 200°C for 1 h in a 20 vol% H_2 and 80 vol% Ar flow (20 mL min^{-1} total, STP) after which the cell was cooled down to 25 °C and purged with a 20 mL min^{-1} (STP) Ar flow for 1 h.

Afterwards, the reaction mixture (35 vol% CH4, 35 vol% CO_2 and 30 vol% Ar; 20 mL min^{-1} total, STP) was introduced into the cell. The catalyst wafer inside the cell was subsequently heated stepwise to 50 °C, 75 °C, 100 °C and 150 °C. For each step the temperature of the wafer was kept constant until steady state was reached (after ± 20

min), after which the temperature was increased to the next step at a heating rate of 3 °C/min.

The catalyst surface (and gas above the surface) was continuously monitored during the DRM reaction using transmission FTIR in the 4000-700 cm^{-1} range with a resolution of 4 cm^{-1} (64 scans per spectrum; 1 spectrum per 5 min). The background spectrum was recorded prior to the introduction of the sample holder with catalyst. The spectrometer was operated using OMNIC software. The results are shown in Figure S39.

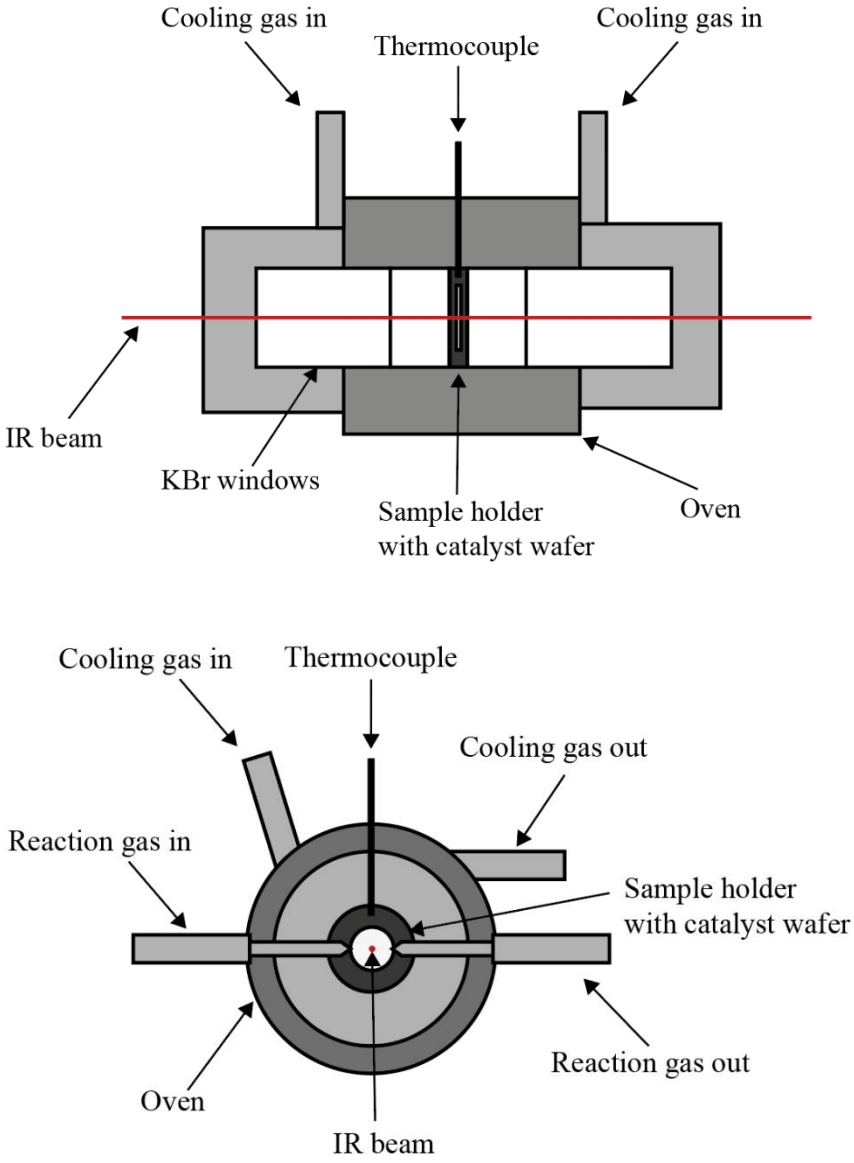

Figure S38: Schematic representation of the front (a) and side (b) view of the thermal *in-situ operando* cell; The cooling gas outlets and reaction gas in- and outlet are perpendicular to the drawing in (a) and thus not illustrated

S6.1. Thermal DRM *operando* IR study

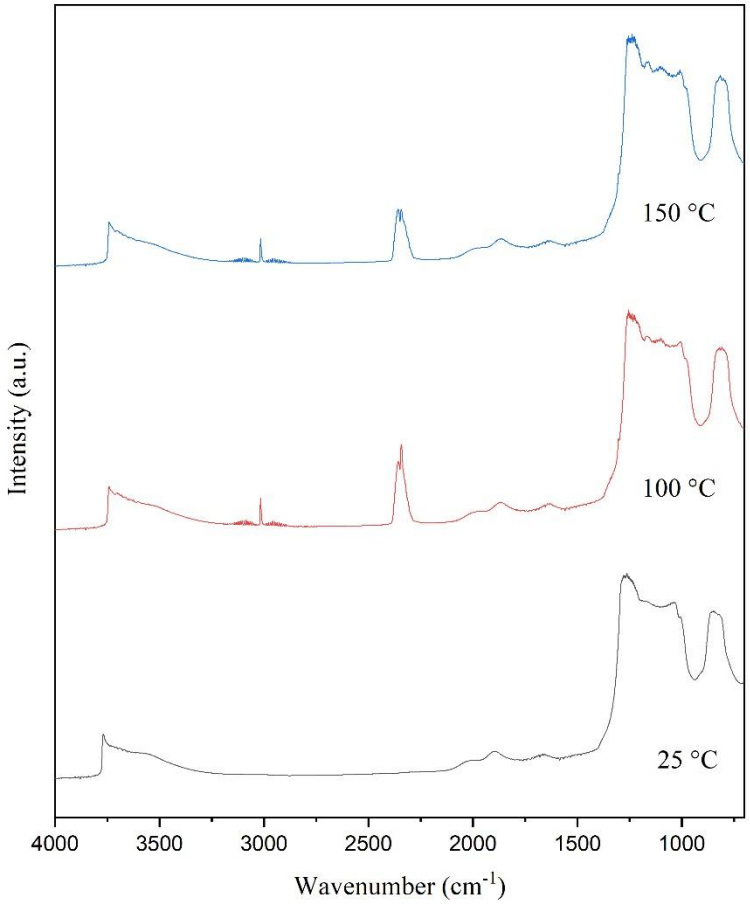

Figure S39: Steady state FTIR spectra (4000-700 cm^{-1}) of the 3 wt% Ru/SiO_2 sample at 25 °C before gas dosing (black) and exposed to a 1:1 CH_4/CO_2 gas mixture in Ar at 100 °C (red) and 150 °C (blue)

Figure S39 clearly shows that at the catalyst surface temperatures observed in the plasma (100-150 °C), no additional bands, representing surface species on the catalyst, are observed, and that no CO is formed. Hence, the formation of surface species and the conversion of CO_2 and CH_4 cannot be attributed to plasma-induced surface heating, but must be due to other plasma-effects such as the adsorption of plasma-generated radicals or molecules, or the occurrence of Eley-Rideal reactions.

S7. Adsorption/desorption of formaldehyde on SiO_2

In order to strengthen the assignment of the band at 1722 cm-1 which we observed during plasma-catalytic DRM on SiO_2, we exposed a SiO_2 sample to formaldehyde, and monitored the desorption behaviour as a function of temperature. Prior to infrared measurements, SiO_2 was activated under secondary vacuum at 200 °C during 1 h. Small formaldehyde volume doses of 2.617 mL were sent to the sample until complete saturation at room temperature (23 °C). The saturation was reached at 240 µmol/g of CH_2O.

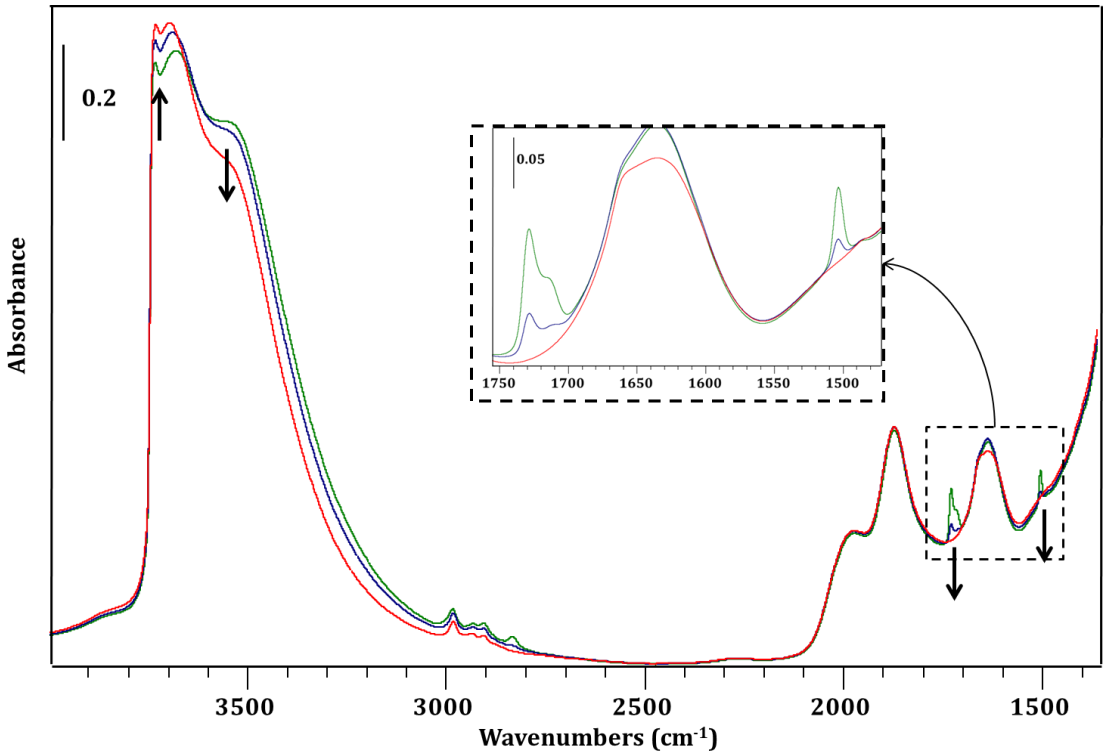

Figure S40: FTIR spectra of physisorbed formaldehyde on SiO_2 at room temperature and ambient pressure (green), after 5 min exposure to secondary vacuum at room temperature (blue) and after 5 min exposure to secondary vacuum at 125 °C (red) in the 4000-1300 cm^{-1} region

References

1. Wuttke, S.; Bazin, P.; Vimont, A.; Serre, C.; Seo, Y. K.; Hwang, Y. K.; Chang, J. S.; Ferey, G.; Daturi, M., Discovering the active sites for C3 separation in MIL-100(Fe) by using operando IR spectroscopy. *Chemistry* **2012,** *18* (38), 11959-67.